



HAL
open science

Numerical investigation of fatigue strength of grain size gradient materials under heterogeneous stress states in a notched specimen

Pierre Baudoin, Vincent Magnier, Ahmed El Bartali, Jean-François Witz, Philippe Dufrenoy, François Demilly, Eric Charkaluk

► To cite this version:

Pierre Baudoin, Vincent Magnier, Ahmed El Bartali, Jean-François Witz, Philippe Dufrenoy, et al.. Numerical investigation of fatigue strength of grain size gradient materials under heterogeneous stress states in a notched specimen. *International Journal of Fatigue*, 2016, 87, pp.132-142. 10.1016/j.ijfatigue.2016.01.022 . hal-01279003

HAL Id: hal-01279003

<https://hal.science/hal-01279003>

Submitted on 15 Jul 2021

HAL is a multi-disciplinary open access archive for the deposit and dissemination of scientific research documents, whether they are published or not. The documents may come from teaching and research institutions in France or abroad, or from public or private research centers.

L'archive ouverte pluridisciplinaire **HAL**, est destinée au dépôt et à la diffusion de documents scientifiques de niveau recherche, publiés ou non, émanant des établissements d'enseignement et de recherche français ou étrangers, des laboratoires publics ou privés.



Distributed under a Creative Commons Attribution 4.0 International License

Numerical investigation of fatigue strength of grain size gradient materials under heterogeneous stress states in a notched specimen

Pierre Baudoin ^{a,*}, Vincent Magnier ^a, Ahmed El Bartali ^a, Jean-François Witz ^a, Philippe Dufrenoy ^a,
François Demilly ^b, Éric Charkaluk ^a

^a Univ. Lille, CNRS, Centrale Lille, Arts et Métiers Paris Tech, FRE 3723 – LML – Laboratoire de mécanique de lille, F-59000 Lille, France

^b MG-Valdunes, Trith St. Léger, France

A possible consequence of forging in common steels is the apparition of a grain size gradient in the width of the component. For railway axles in service, this microstructure gradient is superimposed to the stress gradient introduced by the external load of rotatory bending imposed on the axle. To investigate the combined effects of these gradients on the fatigue lifetime of a forged railway axle, a numerical investigation of the effects of microstructure gradients inserted in a notched specimen is proposed, with respect to different fatigue indicators. In particular, the predictions of an approach based on the theory of critical distances seem to be very promising in this case.

1. Introduction

Ever since the Paris-Versailles accident in the 1840's, railway axles have been a major concern for researchers in the field of fatigue. Due to their loading in rotatory bending, which is in general superimposed in the most critical areas to a local stress gradient induced by notches, they are a typical application of fatigue in the presence of gradients. In the case of forged axles, the macroscopic stress gradients resulting from the external load can be superimposed to microstructural ones, for instance varying grain size in the width of the axle.

Even in the more common case of a homogeneous microstructure, the design of such mechanical parts remains an open problem, as to the authors' best knowledge, there is currently no fatigue criterion that predicts these combined effects in a satisfactory manner. In fact, some of the most frequently used fatigue criteria employed for the design of structures undergoing multiaxial loadings, such as Dang Van's [1] and Crossland's [2] criteria, fail to accurately account for such gradients effects. A wide range of approaches have been attempted to deal with this issue. Papadopoulos et al. [3] proposed a non local-formulation of the Crossland criterion, introducing the gradient of the hydrostatic pressure. This approach was later extended to other criteria by Norberg and

co-workers [4], who underlined, in their case, the better predictability associated with probabilistic approaches. These approaches, built on a weakest link framework [5–7] have gained in popularity, thanks to excellent failure predictions with respect to experiment.

The success of such approaches stems from their capacity to address the random nature of the fatigue phenomenon. From a physical perspective, this randomness is a direct result of heterogeneities present at the microstructure scale (e.g. grain disorientations, inclusions, grain boundaries, defects). However, in most probabilistic approaches this aspect is often masked in macro-scale distributions of fatigue probabilities. In recent years, the emergence of constitutive laws taking into account physical deformation mechanisms at the grain scale ([8,9], for instance) has led to the development of an alternative approach: the statistical study of the fatigue response of polycrystalline aggregates, with respect to some fatigue indicator parameters (FIPs), as introduced by [10] (see [11] for a review). In the case of gradient fatigue, this approach has shown promising results: Bertolino et al. [12] have associated the limitations of Dang Van's criterion with the limited number of grains actually undergoing critical stress in the case of gradient fatigue, and [13] have proposed a statistically defined, microstructure sensitive fatigue notch factor based on numerous aggregates simulations.

The latter category seems entirely indicated to deal with the combined issues of gradient fatigue and heterogeneous underlying

* Corresponding author. Tel.: +33 (0)3 20 33 54 64.

E-mail address: pierre.baudoin@centralliens-lille.org (P. Baudoin).

microstructure, for instance in the case of grain size gradients. For steels, grain size can play an important role in the fatigue life. Some authors [14,15] have found that the fatigue limit could be significantly higher for smaller grain sizes, which they imputed to hardening mechanisms similar to those encountered in monotonic cases. Therefore, to efficiently tackle size effects, the constitutive laws used at the grain scale must be able to reflect hardening mechanisms related to grain size. The crystal plasticity constitutive laws encountered in literature can be divided in two categories: the so-called *phenomenological* approach, based on Cailletaud's [8] work and resting on heuristically defined hardening parameters, and the so-called *physically based* approach [9], which hardening mechanisms are governed by the evolution of parameters such as dislocation densities. The first category is predominant in fatigue studies, and has accumulated significant results, such as the relative importance of elastic anisotropy and crystal plasticity on FIP distributions [16,17], or the importance of local grain cluster effects [18] on individual grain responses. The second category is less encountered in fatigue applications, due to a more difficult identification of the constitutive parameters. Sweeney and co-workers [19] however recently emphasized the relation between local dislocation densities predicted by simulations and experimentally observed crack nucleation on iron oligo-crystals.

Nevertheless, accounting for size effects in a physically consistent manner requires to extend these formulations to non-local descriptions, at a tremendous computational cost. To this day, this approach is mostly limited to simplified microstructures with reduced number of grains [20]. In the case where a macroscopic stress gradient is superimposed to a grain size gradient, over the same characteristic length scale (i.e. covering several hundreds/thousands grains for usual grain sizes, which is the case in a forged railway axle), implementing such non-local constitutive laws remains challenging. The present study aims to circumvent this difficulty by modeling the micro plasticity and hardening mechanisms occurring at the grain scale in a qualitative manner. The proposed approach is to describe individual grain behavior by macroscopic von Mises plasticity models taking the grain size into account to qualitatively reflect grain size effects. This simplification, further discussed in the following sections, seems acceptable if the number of grains involved is sufficiently important.

The present paper is an attempt at characterizing the impact of grain size gradients on the fatigue response of a component subjected to a macroscopic stress gradient. First, a numerical model of this configuration, implementing microstructure gradients on a simplified, axle-representative specimen is proposed. A set of FIPs is then chosen to evaluate the impact of three different microstructure gradients on the fatigue response of the specimen. The relative relevance of these FIPs is then discussed in the final section, and general conclusions on the impact of the microstructures are drawn. In particular, a criterion based on Taylor's theory of critical distances [21] is proposed and reviewed through the prism of aggregate calculations.

2. Numerical model

2.1. Model geometry and mesh

In order to qualitatively assess the mechanical response of polycrystalline aggregates under macroscopical stress gradients, a solution is to place the microstructural gradients at the root of a notched specimen. For a forged axle steel, the microstructural gradient support length is typically the whole width of the component, that is to say, the same support length as the stress gradient. The chosen geometry is then a two-scale model, consisting of a 1 mm × 1 mm patch, inserted at the root of a notched specimen (Fig. 1). The model is two dimensional, and the plane strain

formalism is adopted. The notch geometry, determined by the $\frac{r}{D}$ and $\frac{d}{D}$ ratios, is chosen to reproduce the stress concentration observed on an average railway axle at the fillet joining the wheel seat and the axle body (the previous ratios are identical for the axle and the chosen geometry). On the notched specimen, r is the notch radius, D the width of the specimen, and d the depth of the notch (see Fig. 1). In practice, D is arbitrarily set to 50 mm, and r and d values are deduced from the axle body diameter, wheel seat diameter and fillet radius. For consistency with typical grain sizes encountered in railway steels (about 25 μm), a realistic patch typically contains around 1500 grains.

In practice, the geometry of the specimen is generated extensively with the SALOME Meca software [22], and the aggregate geometry is generated using the Neper software [23]. The resulting multi-scale geometry is then meshed using the netgen algorithm. An example of a mesh produced by this procedure is presented in Fig. 1, with a reduced amount of grains for illustration. The mesh consists of linear triangular elements. For representative aggregates (1500–2000 grains), the mesh contains approximately 150000 elements. Displacement boundary conditions are imposed on the upper and lower surfaces.

This study is limited to two dimensional microstructures. Such aggregates present limitations in the representation of actual microstructures, because at the exception of thin film coatings, in most materials out of plane grain interaction have to be taken into account to model a realistic behavior. Comparison of the surface response of 3D aggregates for different internal grain geometries [24] have shown, however, that the surface strain response is only slightly affected by the underlying microstructure. When considering averaged strain values per grain, the difference is found to be negligible. As the goal here is not so much to try and confirm experimental measurements as to draw general conclusions on the aggregate behavior, limiting the study to 2D aggregates and averaged quantities per grain seems an acceptable compromise.

2.2. Polycrystalline aggregates generation

A common tool of generating virtual microstructures is the use of Voronoi polyhedra, or Voronoi tessellations [25]. Such a tessellation fills the space with no overlaps and no gaps, similarly to a real microstructure. Furthermore, for randomly distributed seeds, the resulting grain size distribution typically exhibits a normal behavior, which is frequently encountered on EBSD (electron backscatter diffraction) cartographies of metallic microstructures [26]. In the case of the axle steel, as a first approximation this kind of tessellation is used.

Voronoi tessellations being completely determined by the position of a given set of seeds, they offer a very easy way to create microstructural gradients. A simple method is to assign each region of the polycrystalline patch a chosen seed density, and to distribute seeds randomly in each region according to this density parameter. It is a simple and convenient way of controlling local grain size while conserving the random geometries associated to Poisson-Voronoi tessellations, and realistic grain geometries.

The chosen approach to distribute seeds can be summed up in three steps:

1. Subdivide the 1 mm × 1 mm patch in a given number of vertical bands where the local grain size will be homogeneous. Arbitrarily, 10 regions are thus defined (defining 100 μm × 1 mm bands, regions significant enough in surface with respect to the average grain size of the considered steels, 30–50 μm).
2. Set a given seed density for each region.
3. Distribute seeds randomly in each region according to the previously determined seed density.

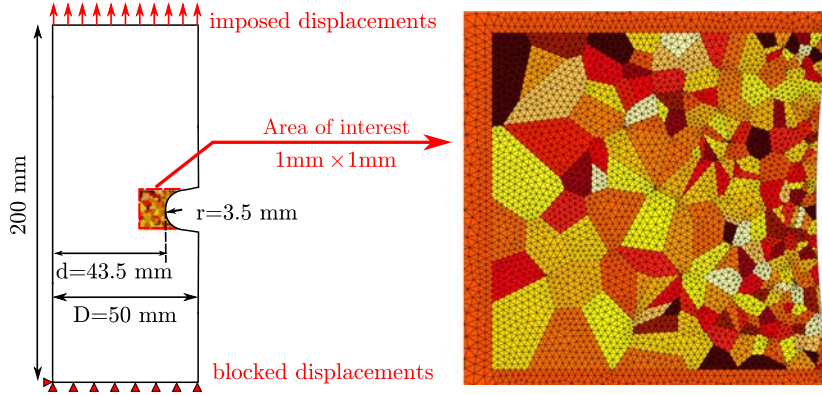


Fig. 1. Multi-scale model and geometry, for a reduced (200) number of grains.

Aggregates obtained through this procedure are presented in Fig. 2, for grain sizes ranging from 10 to 100 μm . Note that the aggregates are generated independently from the macroscopic geometry, into which they are inserted afterwards.

2.3. Constitutive laws

In the chosen model, two scales intervene in the definition of the material response. The macroscopic scale, that describes the behavior of the homogeneous matrix in which the aggregates are to be inserted, and the mesoscopic scale, that describes the individual response of each of the aggregate's grain.

2.3.1. Macroscopic scale

Previous works on the axle steel [27,28] have shown that a constitutive law combining isotropic and kinematic hardening, as described in [29] reflects satisfyingly the cyclic behavior of the material. This law is summarized through equations [(1)–(4)]:

$$\dot{\varepsilon}^p = \dot{\varepsilon}_{eq}^p \frac{\partial f}{\partial \sigma} \quad (1)$$

$$f = J_2(\sigma - X) - R - \sigma_y \leq 0 \quad (2)$$

$$\dot{R} = b(R_\infty - R)\dot{p} \quad (3)$$

$$\dot{X} = \frac{2}{3}C\dot{\varepsilon}^p - \gamma X\dot{p} \quad (4)$$

where the rate of plastic flow $\dot{\varepsilon}^p$ is related to the equivalent plastic strain rate $\dot{\varepsilon}_{eq}^p$ through an associated flow rule. f denotes the yield function and $J_2(\sigma) = \sqrt{\frac{3}{2}}s : s$ is the second invariant of the deviatoric stress tensor $s = \sigma - \frac{1}{3}\text{Tr}(\sigma)I$, and operation “:” denotes the tensor double dot product. The evolution of the elastic domain is governed by the combined evolutions of the isotropic hardening R and the kinematic hardening variable X . This results effectively in a translation and a uniform expansion of the original domain. In addition to the elastic parameters E and ν , five parameters are necessary to implement it in a finite element solver: $\{\sigma_y, R_\infty, b, C, \gamma\}$. σ_y is the

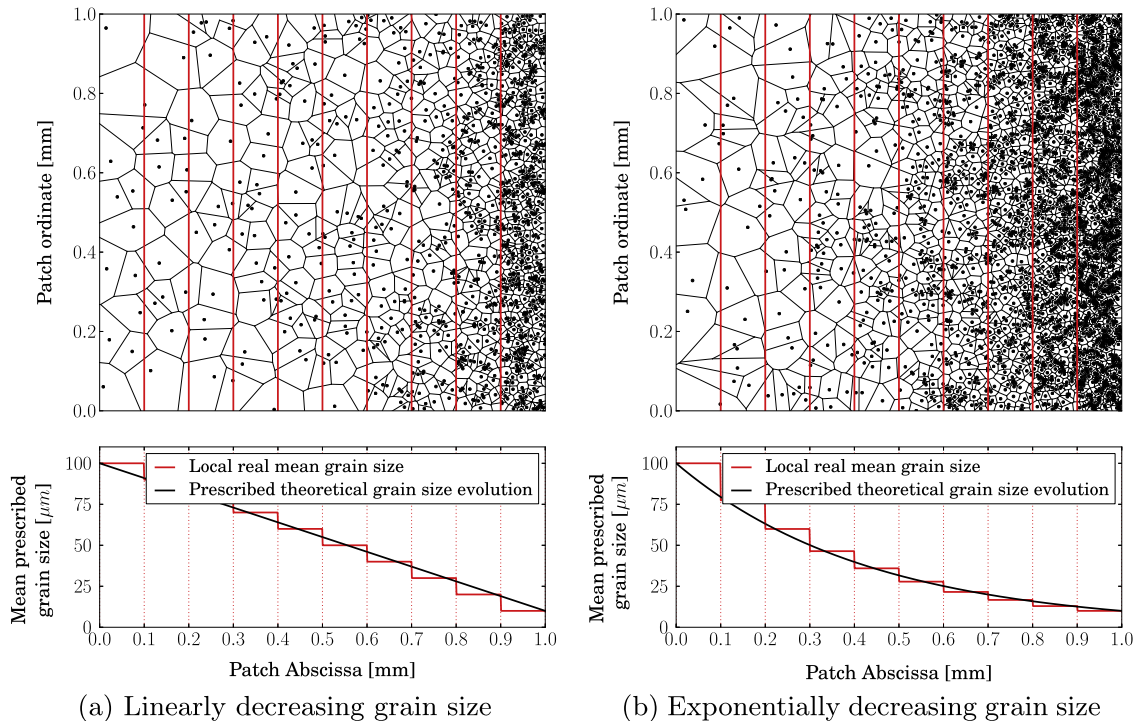


Fig. 2. Microstructural gradient generation: geometry and local grain size evolutions for (a) linear and (b) exponentially decreasing grain sizes in the width of the aggregates.

initial value of R , R_∞ is its asymptotic value, and b allows to control the rate with which R reaches its final value. C is the initial kinematic hardening modulus, and γ is the rate at which it decreases with increasing plastic deformation. The parameters identified by [28] are used here. This constitutive law is affected to all the mesh elements lying outside the polycrystalline aggregate. Note that the matrix behavior will overall remain elastic, save for some elements at the junction with the aggregate.

2.3.2. Mesoscopic scale model

In the case of aggregates with heterogeneous grain sizes, two main microstructural features must be reflected in the description of the mesoscopic response: grain size and grain orientation. Significant progress has been made in recent years to model grain size effects in polycrystals in a physically consistent fashion, using strain gradient plasticity [20,30]. However these models remain computationally expensive, and are so far limited to reduced number of grains. Modeling a grain size gradient, on the other hand, necessitates the explicit modeling of a more important number of grains.

Considering these difficulties, to try and acquire qualitative insight on the combined effects of a grain size gradient and a macroscopic stress gradient on fatigue life, the proposed approach is to model grain orientation and grain size effects in a phenomenological manner, by using the previous macroscopic constitutive law with a different yield stress for each individual grain in the polycrystal. To account for hardening mechanisms related to grain size, as a first approximation, the yield strength $\sigma_{y,g}$ associated to each grain is expressed as a direct function of individual grain size d_g through the empirical Hall–Petch law (Eq. (5)):

$$\sigma_{y,g} = \sigma_0 + \frac{k_y}{\sqrt{d_g}} \quad (5)$$

where σ_0 and k_y are material constants. This empirical law, postulated in the case of monotonic loading, is a traduction of two hardening mechanisms linked to grain size (for a more comprehensive description of grain size effects, see [31]). The first one is an intrinsic grain size effect. For a given grain geometry, a small grain will prove more resilient than a bigger one, because its geometrically necessary dislocation density ρ_{GND} will be more important. The second source of hardening comes from grain boundary hardening: the multiplication of grain boundaries associated with smaller grain sizes effectively limits dislocation movements in the polycrystal (dislocation pile-up effect). One can argue that similar mechanisms take place in the fatigue regime: the multiplication of grain boundaries associated with smaller grain sizes effectively prevents the propagation of microstructurally small cracks (MSC), while higher GND densities effectively slow the formation and subsequent propagation of persistent slip bands. The chosen modeling has the advantage of accounting for both mechanisms, however empirically.

The main hypothesis, as implied by the microstructures generation described on Fig. 2, is that one can consider the grain size gradient as a finite number of bands of homogeneous grain size laid next to each other. When isolating one of these bands, the macroscopic response would then have to comply with the Hall–Petch law if the number of grains in the band is important enough. The chosen modeling can also qualitatively reflect the response of small “clusters” of grains. It is shown in [32] that, within a given aggregate, grain criticality is both a function of grain orientation and grain environment (i.e. surrounding grain size and orientation). The use of macroscopic constitutive laws parameterized with grain size at the grain scale, although not realistic to describe intra-granular fields, is a very simple and efficient way to account for such small clusters effects. Based on a similar modeling, Bertolino

and co-workers [12] underline very clearly the limitations of the Dang Van criterion for heterogeneous loadings. Finally, from an engineering perspective, it is more straightforward to identify the constitutive parameters of macroscopic laws from experimental results, especially in the presence of heterogeneous properties.

As a wide discrepancy can be found in literature for these parameters in steel, it is difficult to come up with a good default value, but according to [33], the Hall–Petch slope k_y can vary between 0.14 and 1.58 MPa m^{1/2} for common steels. The parameters $\{k_y, \sigma_0\}$ are then chosen to reflect a mild steel behavior: $\{\sigma_0 = 100 \text{ MPa}, k_y = 0.8 \text{ MPa m}^{1/2}\}$. As a simplification of the actual steel microstructure, the same couple of parameters is used for all grains in the aggregate, which comes down to assuming that the microstructure is single phase.

2.3.3. Grain orientation

To model grain orientation, a possible methodology is to alter the yield strength obtained for each grain through the Hall–Petch law, by means of a random drawing from a distribution centered around this value. This leads to distribute yield strengths over the aggregate in the three following steps (Fig. 3):

The draw is done from a Gaussian distribution, of mean value $\sigma_{y,g}$, and the standard deviation is taken identical to that of the yield strength distribution given by the Hall–Petch law for a Poisson–Voronoi tessellation of representative grain size. The obtained value, $S = 30 \text{ MPa}$, is in good accordance with a similar modeling realized in [26]. The successive yield strength distributions obtained through this procedure, for an aggregate of approximately 2000 grains are plotted on Fig. 4.

- Fig. 4a shows the initial grain size distribution.
- Fig. 4b shows the yield strength values obtained for that distribution through Eq. (5).
- Fig. 4c shows the final yield strength distribution.

The final yield strength distribution exhibits a typical normal distribution aspect, which is in good accordance with the hypothesis of randomly distributed grain orientations. At this stage, one must verify that the mean response of an aggregate of representative grain size corresponds to the macroscopic steel behavior. To this end, a simple simulation is conducted: a patch of approximately 200 grains is inserted in a plain sample, and the aggregate mean response is compared to the theoretical response given by the macroscopic law for the same load. The results of this simulation are presented on Fig. 5.

The dotted curve presents the macroscopic behavior, and each colored line presents the axial stress response of a grain. It is clear that the mean behavior of the aggregate is very similar to that of the macroscopic model. This simulation supports the assumptions made regarding the distribution of yield strengths.

3. Choice of fatigue indicators

The impact of the grain size variation in the width of the specimen is studied according to the frequential and spatial distribution of several FIPs, described in the next sections. Following the recommendations made in [10], both strain and stress based indicators are considered.

3.1. Crossland's criterion

As a first indicator, the Crossland criterion is considered. This criterion takes into account the magnitude of the octahedral shear

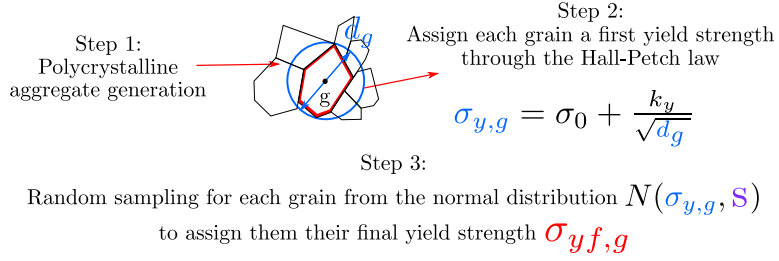


Fig. 3. Mesoscopic yield strengths distribution steps.

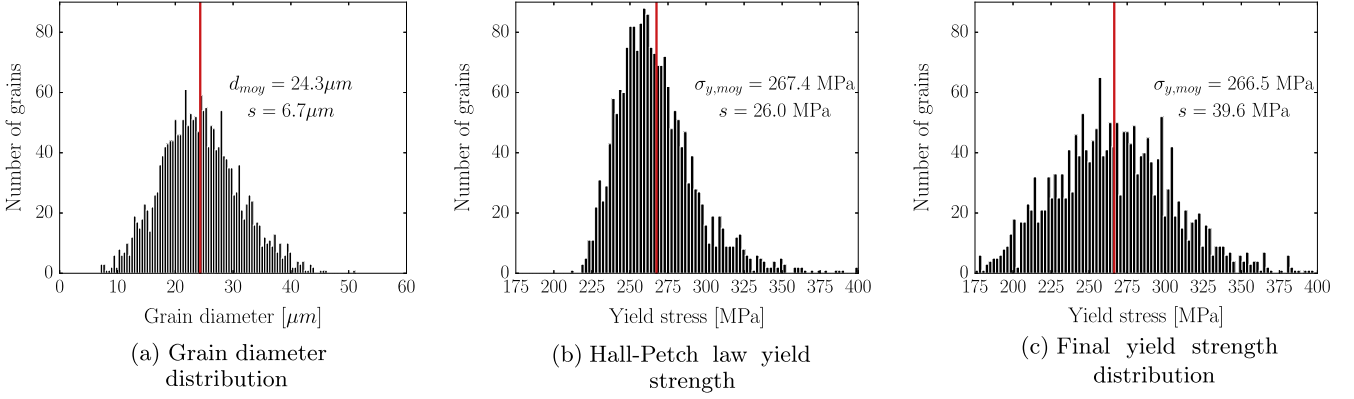


Fig. 4. Yield strengths distribution over the aggregates.

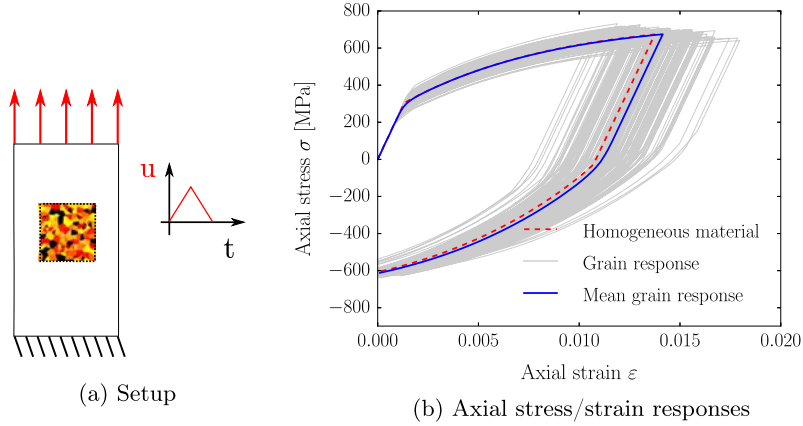


Fig. 5. Overall material behavior compared with the mechanical behavior of each grain.

stress $\sqrt{J_{2,a}}$ and the maximum hydrostatic stress $P_{h,max}$ encountered during a stabilized loading cycle:

$$\sqrt{J_{2,a}} + \alpha P_{h,max} \leq \beta \quad (6)$$

The two coefficients α and β are obtained through fully reversed tensile and torsional fatigue tests:

$$\alpha = \frac{t_{-1} - \frac{s_{-1}}{\sqrt{3}}}{\frac{s_{-1}}{3}}, \beta = t_{-1} \quad (7)$$

where t_{-1} and s_{-1} are respectively the fully reversed tensile and torsional fatigue limits. $\sqrt{J_{2,a}}$ is a measure of the variation of the octaedral shear stress over a stabilized cycle:

$$\sqrt{J_{2,a}} = \frac{1}{2\sqrt{2}} \max_{t_1} \left\{ \max_{t_2} \sqrt{[s(t_2) - s(t_1)] : [s(t_2) - s(t_1)]} \right\} \quad (8)$$

where operation “:” designates the tensor double dot product. The focus will be primarily set on the distribution of both $\sqrt{J_{2,a}}$ and $P_{h,max}$ within the aggregates.

3.2. Cumulated equivalent plastic strain

Many authors [10,16,17,32] insist on the relevance of the equivalent cumulated plastic strain p as a fatigue indicator (Eq. (9)):

$$p = \int_0^t \dot{p} dt \quad \text{with} \quad \dot{p} = \sqrt{\frac{2}{3} \dot{\epsilon}^p : \dot{\epsilon}^p} \quad (9)$$

It is also considered here, as this parameter gives direct insight into the apparition and distribution of plasticity at the mesoscopic scale. It is also shown in [32] that this variable reflects facts observed experimentally, such as a higher failure probability for surface grains.

3.3. Theory of critical distances (point method)

Contrary to the other indicators, the “theory of critical distances” formulated by Taylor [21] is a global criterion, taking into account the stress gradient by averaging the notch stress over a given characteristic length. Three variations are described in [21], according to the space dimension over which the stress (or an equivalent fatigue indicator) is averaged. In the case of a homogeneous grain size, the “point method” involves comparing the stress value at a given depth below the notch with the fatigue limit. In the present case, to account for the effect of varying grain size in the aggregates, a modification of this method is considered here (Fig. 6).

Given the hypothesis made in Section 2.3.2, the main consequence of varying grain size is an associated varying yield strength in the width of the gradient aggregates. To take this fact into account, the equivalent von Mises stress variation will be considered, and compared to the local yield strength in the width of the aggregates. In the case of a homogeneous microstructure (i.e. homogeneous yield strength), this method is equivalent to the original point method. For gradient aggregates, it allows to take into account the hardening induced by varying grain sizes.

For the chosen method, the distance at which the stress is to be considered (denoted $\frac{a_0}{2}$) is given by (Eq. (10)):

$$a_0 = \frac{1}{\pi} \left(\frac{\Delta K_{th}}{\Delta \sigma_0} \right)^2 \quad (10)$$

where K_{th} is the stress intensity threshold beyond which crack propagates, and $\Delta \sigma_0$ is the stress variation at the fatigue limit of a plain specimen. For the railway steel considered here, $\frac{a_0}{2} \approx 0.125$ mm [27].

To the authors’ best knowledge, Taylor’s theory of critical distances has not yet been reviewed through the prism of aggregate calculations. In particular, a long standing question remains the

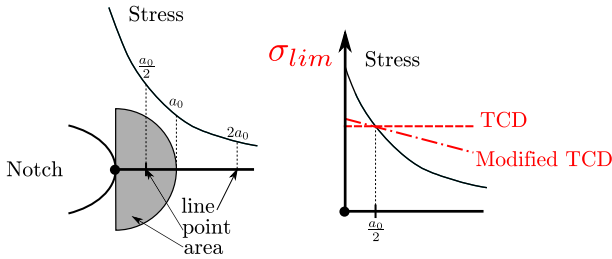


Fig. 6. Theory of critical distances and suggested modification to account for yield strength gradients.

interpretation of this distance can take with respect to the microstructure. This point will be further discussed in the next sections.

4. Microstructures

The three microstructures investigated in this work are depicted in Fig. 7. The corresponding aggregates are noted A_1, A_2 and A_3 in the next sections. The grain size of the first aggregate (A_1) is homogeneous, so that A_1 is later considered as the reference case to calculate the fatigue load. The other two aggregates’ grain size decrease linearly (A_2) and exponentially (A_3) in their width.

The main characteristics of these 3 aggregates are summed up in Table 1. An important distinction must be made at this point considering the evaluations of averaged quantities over these microstructures: whereas averaging over the number of grains and over the area is equivalent for A_1 , significant differences appear in A_2 and A_3 as a consequence of the heterogeneous grain size. This point will be discussed further on because it affects the consideration of the FIP statistical distributions.

4.1. Fatigue load

The fatigue limit is obtained by a calculation on the macroscopic geometry, assuming a purely elastic behavior. The load giving an average stress of 270 MPa (mean yield strength for A_1) over the 1 mm × 1 mm patch in the notch root is considered as the fatigue limit of the A_1 aggregate. For each aggregate, ten cycles are then simulated for this external load. The response of each aggregate, in terms of stabilized axial stress/strain curve is given on Fig. 8. Differences among the three aggregates are already noticeable at this very global scale. The average response of A_3 is entirely elastic, whereas A_1 and A_2 are closer to an accommodated state, with a clear hysteresis for A_2 . From this figure, one can notice that the grain size variations have little impact on the macroscopic response, but can affect significantly individual grain responses. To evaluate grain size effects more precisely, the FIPs distributions at the grain scale must be considered.

5. Results and discussion

5.1. Crossland criterion

The distribution of the Crossland criterion parameters for the three aggregates are given in Fig. 9. The most critical point for aggregate A_1 , is shown by a red dot, and is taken as a reference for comparison. Comparing all three aggregates, the critical value of the Crossland criterion is found to be roughly the same,

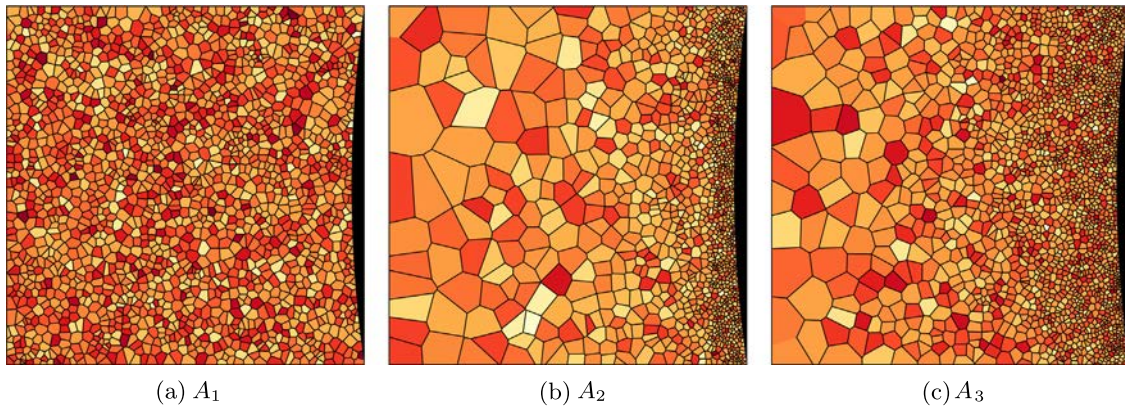


Fig. 7. Modelled aggregates: bulk is on the left, notch on the right.

independently of the grain size distributions. The most critical points are nonetheless obtained for the two aggregates with a microstructure gradient.

Another important point to take into consideration is the distributions of hydrostatic pressure and octaedric shear stress in the aggregates. For most grains in A_2 and A_3 (microstructure gradients), the distributions of these two parameters are clearly bent towards their maximum value, indicating that a high number of grains experience critical loadings with regards to the Crossland criterion. On the other hand, the opposite phenomenon is observed for A_1 , with a very reduced number of grains actually critical with regards to this fatigue criterion.

Finally, the spatial variation of the scatter obtained on the values of the Crossland criterion (see the indicated areas on Fig. 9a-c) yields important information. Given the chosen constitutive laws, isotropic, this scatter is necessarily related to the onset of plasticity in some grains. For the homogeneous aggregate A_1 , plasticity is essentially confined to the notch root, with a purely elastic behavior for the bulk grains. The opposite situation is observed for

the remaining two aggregates, in which scatter in the criterion values occurs mostly for the bulk grains. This is a direct consequence of the yield strength gradient existing between the surface and the bulk of aggregates A_2 and A_3 .

These considerations illustrate the fact, very well shown in [10,32] for instance, that a fatigue criterion based purely on stress is a poor indicator of fatigue severity at the mesoscopic scale. Following these authors, the distribution of cumulated plastic strain seems to be a more consistent choice.

5.2. Cumulated plastic strain

The distributions of p in Fig. 10 confirm the spatial localizations of plasticity deduced from the Crossland diagrams, with very clear differences with regards to the underlying microstructures.

Differences in the plastified volumes are inferred from these distributions. To distinguish plastified volume and plastified microstructure fraction (relative number of grains), the corresponding distributions are plotted in Fig. 11.

For A_1 (homogeneous grain size), there is no significant difference in the volumic and microstructural distributions. However, for the other two aggregates, significant differences in these distributions underline that an average per grain underestimates the importance of the damage. For the lower values of p ($0.0 \leq p \leq 0.01$), the volumic fractions of A_2 are indeed more important than A_1 , implying a much more important overall plastified volume (see Table 2). However, the most important value of p is encountered in A_1 , for the homogeneous grain size.

In order to assess the distributions of p near the maximum values for the three cases, the associated repartition functions are plotted in Fig. 11d. This figure shows a clearly positive impact of

Table 1
Grain size and yield strengths of the three aggregates: mean values and standard deviations evaluated per grain and per unit of surface.

	Aggregate 1	Aggregate 2	Aggregate 3
Number of grains	1974	1385	2118
d_{av} [μm]	24	21	20
μ_d [μm]	6.8	21	15
$\sigma_{y,av}$ [MPa] (per grain)	270	310	310
μ_{σ_y} [MPa] (per grain)	45	110	120
$\sigma_{y,av}$ [MPa] (per unit of surface)	236	195	219
μ_{σ_y} [MPa] (per unit of surface)	6	50	51

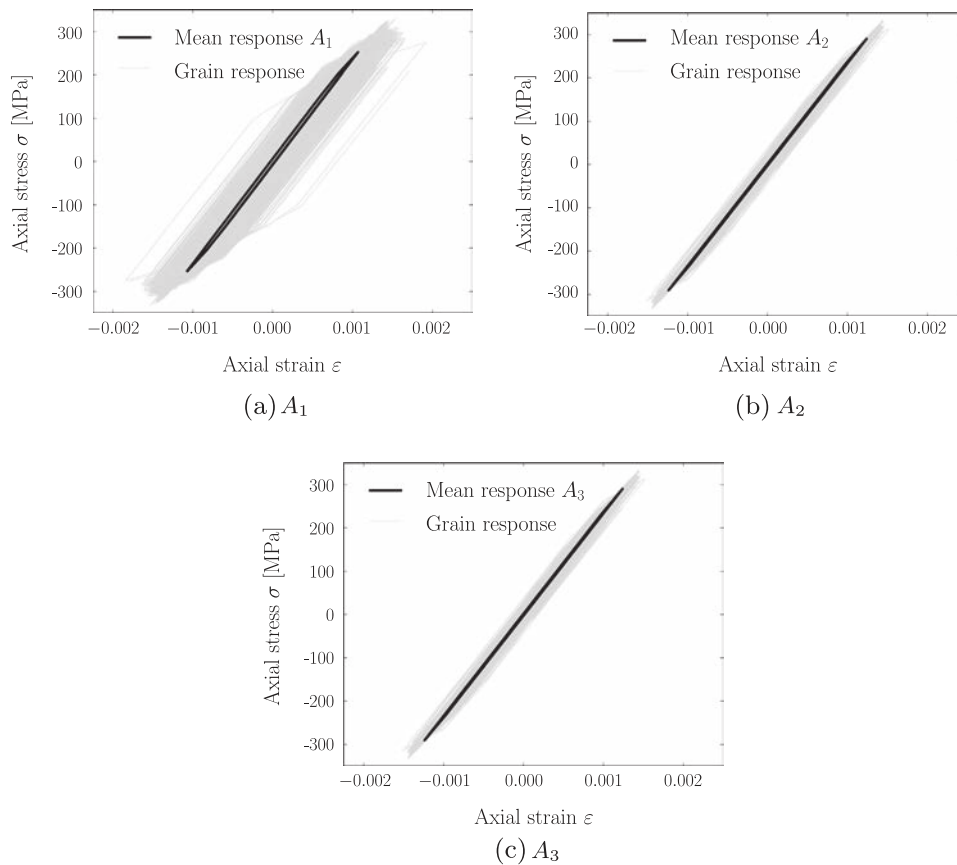


Fig. 8. Stabilized stress strain/cycles at the mesoscopic and macroscopic scales for the three aggregates: (a) A_1 , (b) A_2 and (c) A_3 .

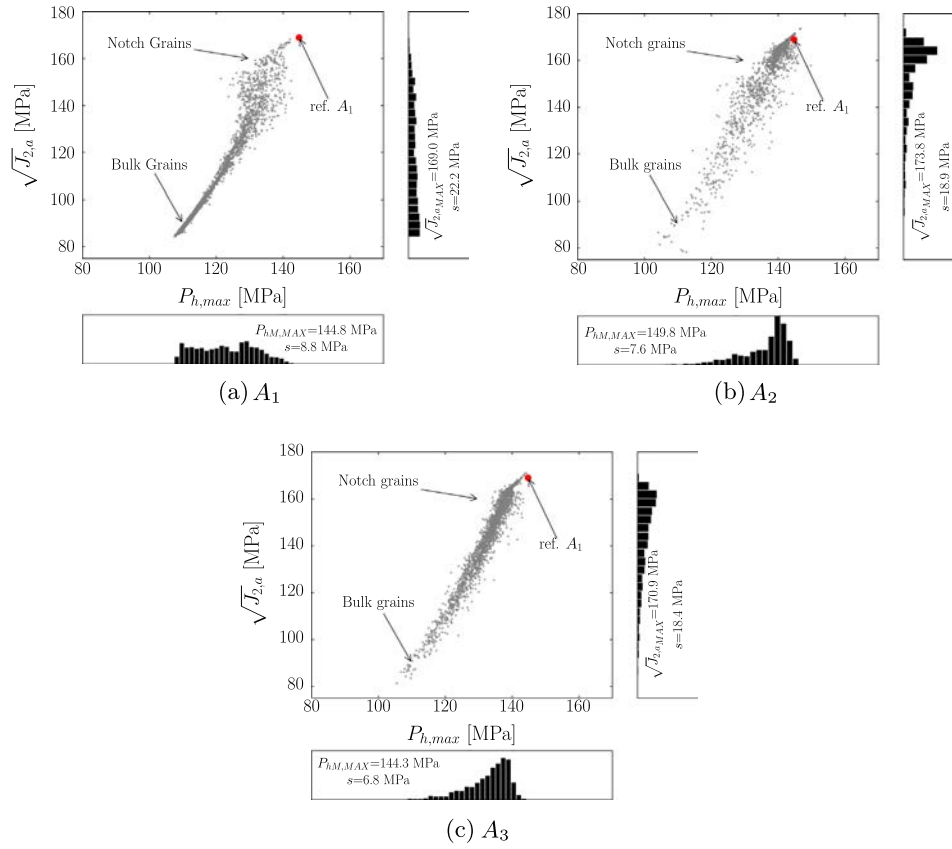


Fig. 9. Crossland criterion evaluated on each grain on the last loading cycle and corresponding distributions of octahedral shear stress and maximum hydrostatic stress for the three aggregates: (a) A_1 , (b) A_2 and (c) A_3 .

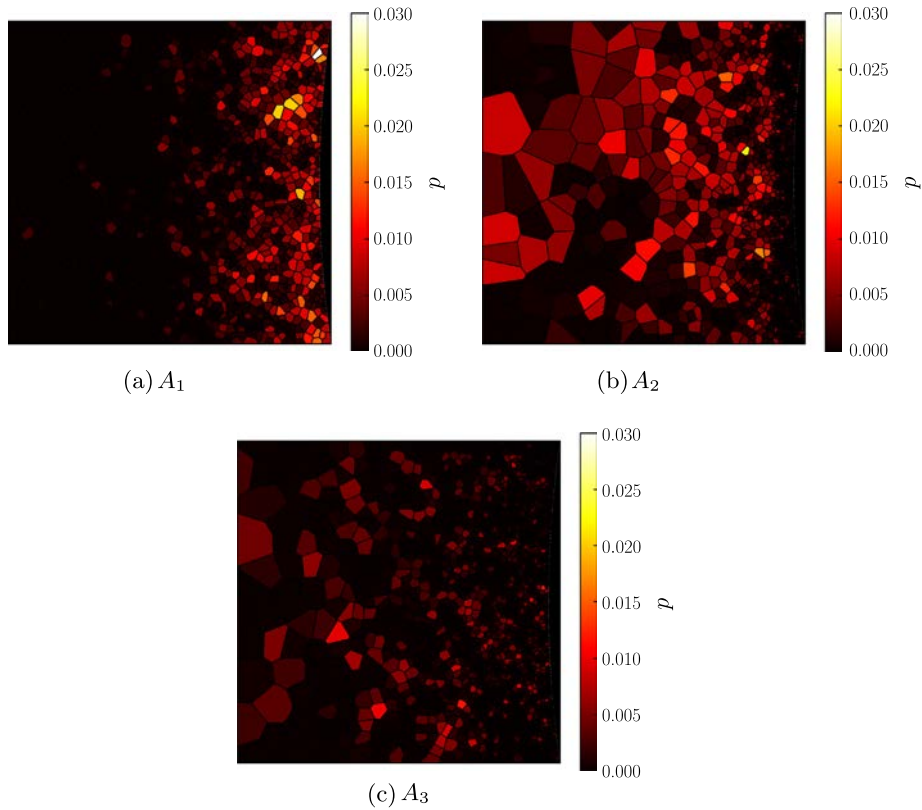


Fig. 10. Cumulated equivalent plastic strain p (average per grain) after 10 cycles for the three aggregates: (a) A_1 , (b) A_2 and (c) A_3 .

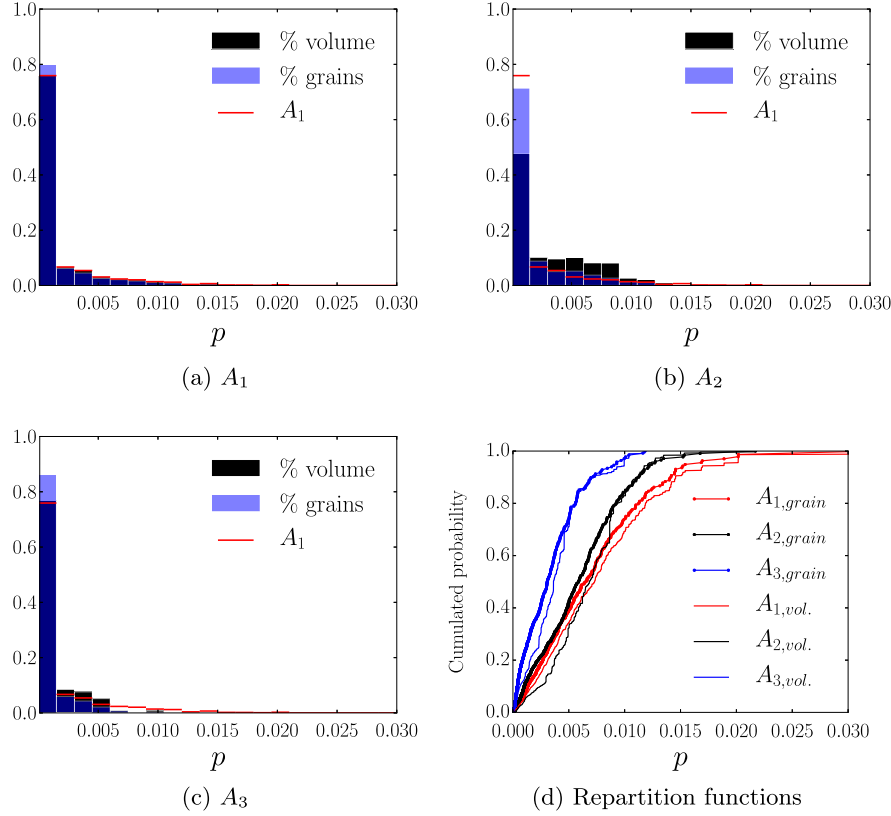


Fig. 11. Plastic strain distributions as volumic and grain fractions for the three aggregates (a) A_1 , (b) A_2 , (c) A_3 and (d) corresponding repartition functions.

Table 2

Plasticity distribution over the three aggregates: maximum value, average per grain, average per element of volume and corresponding plastified fractions over the aggregates.

	A_1	A_2	A_3
p_{max}	0.03213	0.02171	0.01183
$p_{mean,g}$	0.00124	0.001721	0.00071
$p_{mean,vol}$	0.00153	0.00325	0.00110
Plastified grains (%)	25	35	17
Plastified volume (%)	29	59	29

the microstructural gradients with regards to plasticity, as the tails of the repartition functions are shifted to lower strain values for the gradient aggregates. Table 2 sums up the data regarding cumulated plastic strain. Note that the plastified volume fractions are expressed over the aggregate volume, and that the specimen response outside the aggregate is entirely elastic, save for a few elements lying on the boundary of the aggregates. As a result, plasticity is essentially confined to a very small volume, as expected in the high cycle fatigue regime.

Regardless of the considered variable, aggregate A_3 exhibits the least critical response. Distinguishing between the remaining two aggregates is however non-trivial, and would require some experimental insight. The spread of plasticity is more pronounced for aggregate 2, whereas it is really confined for aggregate 1. However, the few grains that plastify in the latter case exhibit much more important values of p than for the second aggregate. These two aggregates lie in an undetermined situation, both considering mean values (Table 1) and the local distributions.

5.3. Prediction given by a critical distance approach

To evaluate the average stress at the depth of the critical distance (point method, $\frac{a_0}{2} = 0.125$ mm) in the different aggregates,

the variation of the averaged von Mises stress in the width of the three aggregates is plotted in Fig. 12 (denoted $\sigma_{vm,mean}(A_i), i = 1 \dots 3$, black curves). The average yield strength at a given depth is also represented (denoted $\sigma_{y,mean}(A_i), i = 1 \dots 3$, red curves).

For the three aggregates, the perceived macroscopical von Mises stress is near-identical, independently of the local grain size, and the stress at the critical distance is 275 MPa (close to the supposed fatigue limit of the homogeneous grain-size aggregate). For A_3 , the local yield strength in $\frac{a_0}{2}$ is superior to the applied stress. In that case, T.C.D. indicates that the applied load on the aggregate is below its fatigue threshold, which is in agreement with the stabilized stress-strain curves and the plasticity distributions. For the

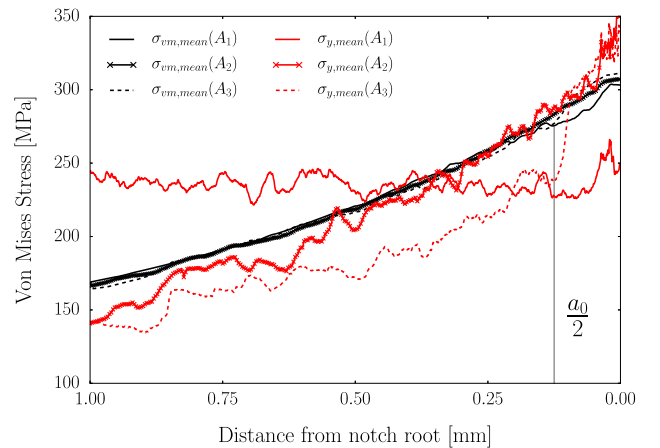


Fig. 12. von-Mises stress (black) and local yield stress (red) variations in the width of the aggregates. (For interpretation of the references to colour in this figure legend, the reader is referred to the web version of this article.)

remaining two aggregates however, the local yield strength is below the macroscopic load, pointing toward a solicitation beyond their respective fatigue limit. An interesting point is that for both A_1 and A_2 , the local yield strengths in $\frac{a_0}{2}$ are very close (approx. 235 MPa), and that it is also difficult to tell them apart from a micro-damage localization point of view (see Table 2 and Fig. 11).

The interest of the T.C.D. is that it yields the same qualitative conclusions as the cumulated plastic strain indicator at the smaller scale of the microstructure, while considering only averaged stresses. The location of the most critical areas in each aggregate can also be easily deduced from the comparison of local yield strength and applied stress (Fig. 12). Finally, one can notice that the value of the critical distance in this configuration is of the same order of magnitude as a few times the grain size. Given the previous remarks, this seems to indicate that the whole aggregate response can be determined by the response of the smaller number of grains lying in the critical distance area.

5.4. Overview

In the chosen framework, all three FIPs are relevant to access some information considering the fatigue behavior of the microstructures. In the case of the Crossland criterion, however, one should note that the interpretation of the figures would have been significantly more complicated for more realistic mesoscopic constitutive laws (see [16,17] in particular, who show the crucial importance of elastic anisotropy on the obtained FIP scatter). For this category of constitutive laws, using the mesoscopic variations of this criterion to assess local plasticity in microstructure gradients would prove inappropriate.

Generally speaking, the richest information is obtained by the study of the distributions of plastic strain in the aggregates. For strong grain size gradients, this indicator has shown that averaging FIPs over the total number of grains instead of the total volume can lead to underestimate the actual spread of plasticity in the presence of varying grain size. On another hand, the theory of critical distances is an approach that is currently widely used in the engineering world for fatigue lifetime estimation. The predictions of the modified T.C.D. proposed in this work seem promising in the case of microstructural gradients. The chosen comparison between local yield strength and applied stress indicates a competition mechanism between the stress variations and the grain size variation. This simplified consideration reveals several aspects confirmed at the smaller scales by the other FIPs:

- Plasticity location differ significantly in the presence of microstructure gradients (localized in the bulk, whereas in the notch tip for the homogeneous aggregate).
- The most critical values for p are found in A_1 .
- Aggregate A_3 has an optimized grain size variation with respect to the macroscopic load.

All these three considerations can be drawn from the sole consideration of averaged quantities over the aggregates, which is interesting from an engineering perspective.

The positive effect of grain size variations of aggregates has also been underlined, as in the proposed framework, the most severely loaded areas also had the highest yield strengths. In this case, crack initiation below the surface is expected to take place as a possible consequence of these microstructure gradients.

6. Conclusion

This study has addressed the combined effects of stress gradients and heterogeneous material properties in a notched specimen

in the fatigue regime by studying the distributions of several FIPs with respect to different microstructures. On the basis of a phenomenological model, several conclusions have been drawn about the possible consequences of the introduction of a varying grain size in the width of the specimen. Using traditional stress based fatigue criteria such as Crossland and Dang Van would prove inappropriate in the presence of a grain-size gradient. The systematic study of plastic strain distributions seems a more promising perspective. The encouraging predictions made in the critical distance framework proposed in this work indicate that non-local global approaches could remain relevant to tackle the many issues dealt with in the problem at hand. In the case of a forged railway axle, using such a global criterion also seems a more viable solution from an engineering perspective.

The perspectives of this work are both numerical and experimental. Strain gradient plasticity models would give further insight on the response of microstructure gradients, under homogeneous or heterogeneous loads. In this study, residual stress have not been considered, but could also significantly impact the fatigue behavior of forged axles. Further experimental campaigns on such materials would also yield interesting conclusions, especially regarding the crack initiation location.

Acknowledgements

The InnovAxle project has been funded by the Nord-Pas-de-Calais Region, the European Community and the BPIFrance. The authors gratefully acknowledge the support of these institutions.

References

- [1] Van KD. Sur la résistance à la fatigue des métaux. Ph.D. thesis, In Sciences et Techniques de l'Armement; 1973.
- [2] Crossland B. Effect of large hydrostatic pressures on the tensional fatigue strength of alloy steel. In: Proceedings of the international conference on fatigue of metals; 1956. p. 138–49.
- [3] Papadopoulos IV, Panoskaltis VS. Invariant formulation of a gradient dependent multiaxial high-cycle fatigue criterion. Eng Fract Mech 1996 (55):513–28.
- [4] Norberg S, Olsson M. The effect of loaded volume and stress gradient on the fatigue limit. Int J Fatigue 2007(29):2259–72.
- [5] Delahay T, Palin-Luc T. Estimation of the fatigue strength distribution in high-cycle multiaxial fatigue taking into account the stress-strain gradient effect. Int J Fatigue 2006(28):474–84.
- [6] Morel F, Huyen N. Plasticity and damage heterogeneity in fatigue. Theor Appl Fract Mech 2008;49(1):98–127.
- [7] Härkegard G, Halleraker G. Assessment of methods for prediction of notch size effects at the fatigue limit based on test data by Böhm and Magin. Int J Fatigue 2010(32):1701–9.
- [8] Cailletaud G, Doquet V, Pineau A. Cyclic multiaxial behaviour of an austenitic stainless steel: microstructural observations and micromechanical modelling. In: Fatigue under biaxial and multiaxial loading, MEP; 1991. p. 131–49.
- [9] Dunne F, Rugg D, Walker A. Lengthscale-dependent, elastically anisotropic, physically-based hcp crystal plasticity: application to cold-dwell fatigue in ti alloys. Int J Plast 2007;23(6):1061–83.
- [10] Bennett V, McDowell D. Polycrystal orientation distribution effects on microslip in high cycle fatigue. Int J Fatigue 2003;25(1):27–39.
- [11] McDowell D, Dunne F. Microstructure-sensitive computational modeling of fatigue crack formation. Int J Fatigue 2010;32(9):1521–42.
- [12] Bertolino G, Constantinescu A, Ferjani M, Treiber P. A multiscale approach of fatigue and shakedown for notched structures. Theor Appl Fract Mech 2007 (48):140–51.
- [13] Owolabi G, Prasannavenkatesan R, McDowell D. Probabilistic framework for a microstructure-sensitive fatigue notch factor. Int J Fatigue 2010;32 (8):1378–88.
- [14] Di Schino A, Kenny M. Grain size dependence of the fatigue behaviour of a ultrafine-grained aisi 304 stainless steel. Mater Lett 2003(57):3182–5.
- [15] Park J, Kim S, Kim K, Park S, Lee C. A microstructural model for predicting high cycle fatigue life of steels. Int J Fatigue 2005(27):1115–23.
- [16] Robert C, Saintier N, Palin-Luc T, Morel F. Micro-mechanical modelling of high cycle fatigue behaviour of metals under multiaxial loads. Mech Mater 2012 (55):112–29.
- [17] Guerchais R, Saintier N, Morel F, Robert C. Micromechanical investigation of the influence of defects in high cycle fatigue. Int J Fatigue 2014;67:159–72.

- [18] Guilhem Y. Numerical investigation of the local mechanical fields in 316L steel polycrystalline aggregates under fatigue loading. Ph.D. thesis, Mines ParisTech; 2011.
- [19] Sweeney C, Vorster W, Leen S, Sakurada E, McHugh P, Dunne F, et al. The role of elastic anisotropy, length scale and crystallographic slip in fatigue crack nucleation. *J Mech Phys Solids* 2013;61(5):1224–40.
- [20] Sweeney C, O'Brien B, Dunne F, McHugh P, Leen S. Strain-gradient modelling of grain size effects on fatigue of cocr alloy. *Acta Mater* 2014;78:341–53.
- [21] Taylor D. Geometrical effects in fatigue: a unifying theoretical model. *Int J Fatigue* 1999(21):413–20.
- [22] Salome-meca. <<http://www.salome-platform.org/>>.
- [23] Quey R, Dawson P, Barbe F. Large-scale 3d random polycrystals for the finite element method: generation, meshing and remeshing. *Comput Methods Appl Mech Eng* 2011(200):1729–45.
- [24] Heripre E. Méthode de couplage multi-échelles entre simulations numériques polycristallines et mesures de champs pour l'identification des paramètres de lois de comportement et de fissuration des matériaux métalliques. Ph.D. thesis, École Polytechnique; 2006.
- [25] Cailletaud G, Forest S, Jeulin D, Feyel F, Galliet I, Mounoury V, et al. Some elements of microstructural mechanics. *Comput Mater Sci* 2003(27):351–74.
- [26] Seghir R, Bodelot L, Charkaluk E, Dufrénoy P. Numerical and experimental estimation of thermomechanical fields heterogeneity at the grain scale of 316L stainless steel. *Comput Mater Sci* 2012;53(1):464–73.
- [27] Gros V. Étude de l'amorçage et de la propagation des fissures de fatigue dans les essieux-axes ferroviaires. Ph.D. thesis, École Centrale Paris, 1996.
- [28] Yameogo A. Étude expérimentale et numérique de l'amorçage et de la propagation de fissures de fretting dans un assemblage roue/essieu ferroviaire. Ph.D. thesis, Université Paul Sabatier de Toulouse III; 2004.
- [29] Lemaitre J, Chaboche J. Mécanique des matériaux solides. Dunod; 2001.
- [30] Cordero N, Forest S, Busso EP, Berbenni S, Cherkaoui M. Grain size effects on plastic strain and dislocation density tensor fields in metal polycrystals. *Comput Mater Sci* 2012;52(1):7–13.
- [31] Zhu T, Bushby A, Dunstan D. Materials mechanical size effects: a review. *Mater Technol* 2008;23(8):193–209.
- [32] Guilhem Y, Basseville S, Curtit F, Stephan J-M, Cailletaud G. Investigation of the effect of grain clusters on fatigue crack initiation in polycrystals. *Int J Fatigue* 2010;32(11):1748–63.
- [33] Lim H, Lee M, Kim J, Adams B, Wagoner R. Simulation of polycrystal deformation with grain and grain boundary effects. *Int J Plast* 2011;27(9):1328–54.